Geological Society, London, Special Publications

Thermal expansion and its control on the durability of marbles

Annette Zeisig, Siegfried Siegesmund and Thomas Weiss

Geological Society, London, Special Publications 2002, v.205; p65-80.
doi: 10.1144/GSL.SP.2002.205.01.06

Notes

Thermal expansion and its control on the durability of marbles

ANNETTE ZEISIG, SIEGFRIED SIEGESMUND & THOMAS WEISS
Geowissenschaftliches Zentrum der Universität Göttingen, Goldschmidtstrasse 3,37077 Göttingen, Germany (e-mail: tweiss@gwdg.de)

Abstract: Marbles as ornamental stones as well as in their natural environments show complex weathering phenomena. The physical weathering of marbles due to thermal treatment is often discussed as the initial stage of deterioration. Eighteen different well-known marble types were selected to quantify experimentally the effect of heating and cooling within the temperature range of 20°C to 85°C while three different ramps at 40°C, 60°C and 85°C were performed. The marbles differ in composition from calcitic to dolomitic as well as in their fabrics. The average grain size varies from 50 μm up to 3 mm, while the grain boundary geometry differs from a granoblastic foam structure to those with weakly inequigranular-amoeboid structure. The lattice preferred orientations are also highly different in c-axis and a-axis distributions. With respect to the heating and cooling cycles three distinct groups of marbles can be distinguished: Type I is characterized by an isotropic thermal expansion (α) and large isotropic residual strain (permanent length changes); Type II exhibits an anisotopic α and no or small isotropic residual strains; while Type III shows an anisotropic α and anisotropic residual strain. Most samples show deteriorations due to thermal treatment, which cannot be uniformly explained without taking into account the rock fabrics. The magnitude and directional dependence of the thermal expansion is mainly controlled by the lattice and shape preferred orientation. The composition, grain size, grain boundary geometry and pre-existing microcracks modify in a more complex way the progressive loss of cohesion due to dilatancy caused by the anisotropic thermal expansion.

Over the last few decades, many field and laboratory studies have shown that marble shows a very special weathering behaviour and, moreover, the important mechanisms of rock decay in a range of environments are still under discussion (Fig. 1).

The high reactivity of calcite and dolomite in humid environments is well known. Solution, precipitation, alteration and corrosional phenomena, including stress-induced ones, represent the largest variety of chemical and biological action (Lasaga & Blum 1986; Watson & Brenan 1987; MacInnis & Brantley 1992; Schwarz *et al.* 1991*a*, *b*; Simon & Snethlage 1993).

The progressive loss of cohesion along grain boundaries is often discussed as an initial stage of marble decay caused by physical weathering. Kessler (1919) found that repeated heating and cooling may lead to permanent length changes, and therefore to changes in the microfabric. These observations were confirmed by many researchers. Rosenholtz & Smith (1949), Zezza *et al.* (1985), Grimm & Schwarz (1985), Sage (1988), Watson & Brenan (1987), Grimm (1999). Thomasen & Ewert (1984), Monk (1985), Bortz *et al.* (1988), Poschlod (1990) and Winkler (1996) all concluded that a variation in moisture content controls decay in marbles. Poschlod (1990) found a maximum value of 100 μm/m for the hygric expansion of Carrara marble, while Grimm (1999) reported length changes up to 1 mm/m. The highly anisotropic thermal expansion of calcite, and the less pronounced expansion in dolomite, is frequently discussed as the main driving force of marble deterioration. Rosenholtz & Smith (1949), Sage (1988), Franzini (1995) and Widhalm *et al.* (1996) reported length changes of 1 mm/m due to heating and cooling. Thermally treated marbles, which do not return to the initial length change after cooling, can show a residual stress even as a result of very small temperature changes between 20 and 50°C (Battaglia *et al.* 1993). Widhalm *et al.* (1996), Tschegg *et al.* (1999) and, more quantitatively, Siegesmund *et al.* (2000*a*, *b*) show that the rock fabric has a significant influence on the distinct differences in weathering of marbles, although they are of nearly identical compositions. The rock fabric includes the grain size, grain boundary geometry, shape preferred orientation, lattice preferred orientation (here referred to as texture) and pre-existing microcracks.

To demonstrate the importance of rock fabrics on physical weathering due to thermal expansion, a large collection of marbles was selected. The marbles differ in composition,

From: SIEGESMUND, S., WEISS, T. & VOLLBRECHT, A. 2002. *Natural Stone, Weathering Phenomena, Conservation Strategies and Case Studies*. Geological Society, London, Special Publications, **205**, 65–80.
0305-8719/02/$15.00

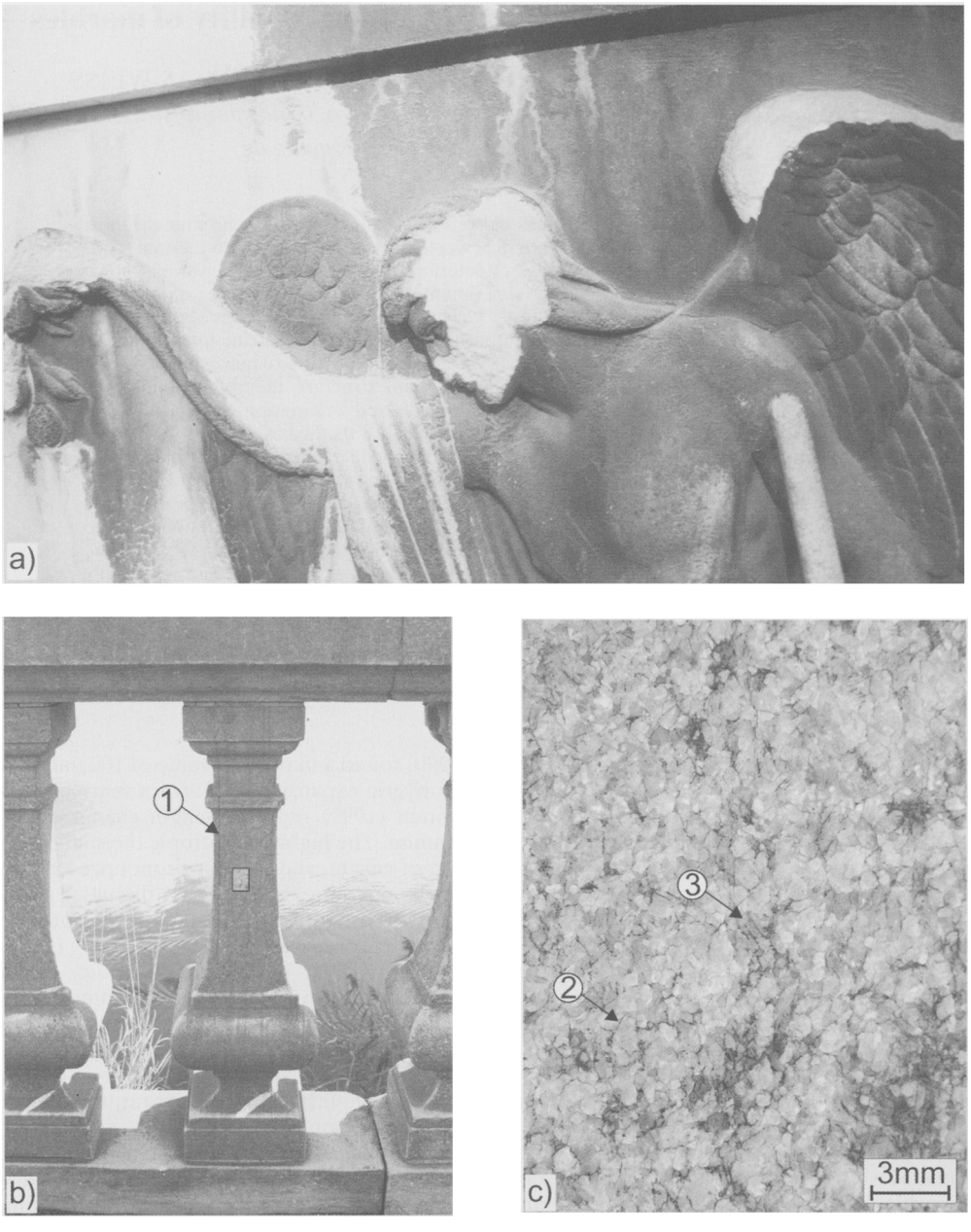

Fig. 1. Weathering of marble. (**a**) A relief at the Südfriedhof in Munich showing granular disintegration, backweathering and loss of relief structure. (**b**) Baluster from the Marmorpalais in Potsdam, rock type Grosskkunzendorf marble. A vertical foliation acts as a preferred zone of weakness leading to penetrating fractures (1). (**c**) Detail from (b): a certain amount of degradation is visible by microbial fouling preferentially along the grain boundaries (2) but also along intragranular (3) planes (e.g. cleavage planes).

grain size, shape fabrics and texture. Based on texture analyses of calcite and dolomite, the directional dependence of thermal dilatation was modelled and quantitatively compared with the experimental data. Emphasis is placed on the extent to which each fabric element in the polycrystalline marble controls the residual strain to characterize the effect of stone decay.

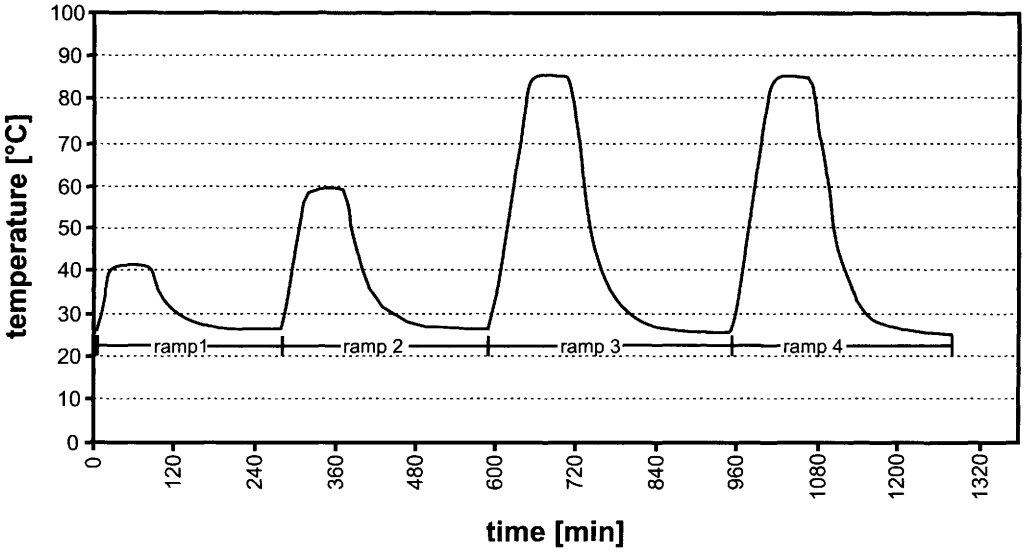

Fig. 2. Temperature pattern of the ramps performed in the thermal dilatation measurements. Heating was performed at a rate of 1°C/min. The destination temperatures are 40°C (ramp 1), 60°C (ramp 2) and 85°C (ramps 3 and 4).

Experimental

Thermal expansion measurements were performed by using a triple dilatometer (for details see Widhalm *et al.* 1996). The sample size corresponds to a cuboid of 10 × 10 × 50 mm. Calibration of the dilatometer was done using quartz glass, and the final displacement resolution was better than 1 μm. Due to a sample length of 50 mm a final residual strain of about 0.02 mm/m could be resolved. This setup allows the simultaneous measurement of the thermal expansion anisotropy of three specimens at identical experimental conditions. Thermal dilatation is a property which can be described by a second rank tensor. To quantify an arbitrary orientation of a second rank tensor, measurements in six independent directions were performed (see Siegesmund *et al.* 2000*b*).

In order to simulate temperature changes comparable to those observed under natural conditions for building or ornamental stones, the upper temperature limit was fixed at 85°C. Heating was performed with a velocity of 1°C/min to ensure thermal equilibration of the specimen. Thermal degradation may occur at significantly lower temperatures than 85°C. Thus, different ramps were driven in the thermal dilatation measurements (Fig. 2). The first ramp was up to about 40°C. After reaching the destination temperature, this temperature was kept stable until the continuous expansion of the sample vanished. Then, the specimen was cooled to room temperature. The same sequence was applied for the second ramp (60°C) and third ramp (85°C). Generally it was observed that the slope of the curves was small in ramps 2 and 3 until the end of the previous ramp was reached. Then, the slope increased significantly. The last ramp up to 85°C was repeated to investigate whether the samples are continuously degraded or the residual strain is only a phenomenon observed for one-off heating to a certain destination temperature. Different units are used for the description of thermal expansion and residual strain. The thermal dilatation coefficient α is calculated as the ratio between the length change of the sample Δl and the original sample length l multiplied by the temperature interval ΔT in kelvin ($\alpha = \Delta l/(l \times \Delta T)$). The corresponding unit is 10^{-6} K^{-1}. In contrast, the residual strain ε (in mm/m) is defined as the ratio between the length change of the sample Δl and the original sample length l. Thus, values for the residual strain can only be directly compared within the same ramp.

For the texture measurements neutron diffraction was applied. The analysis was carried out at the time-of-flight (TOF) neutron diffractometer NSHR, which is located at the pulsed reactor IBR-2 of the Frank Laboratory for Neutron Physics in Dubna, Russia (for the

Table 1. *Fabric of the marbles investigated*

Marble	Abbr.	Fabric	Grain size	SPO	Comp.	mrd	TD-type
Carrara	C1	inequigranular-polygonal	200 μm (50–100 μm)	+	cc	1.42	I
Carrara	C2	inequigranular-polygonal	300 μm (100–200 μm)	+	cc	1.46	I
Diamant	D1	equigranular-interlobate	2–3 mm	+	cc	2.96	III
Arabella	GA	equigranular-polygonal	100 μm	–	do	1.33	I
Grosskunzendorf	GK	equigranular-interlobate	1.5 mm	–	cc	2.35	II
Gitano	GT	seriate-polygonal	50 μm	0	cc	2.47	II
Thassos	GTH	equigranular-interlobate	1.75 mm	+	do	7.00	II
Volakas	GV	inequigranular-polygonal	75–100 μm	+	cc	2.58	III
Lasa	LA1	inequigranular-interlobate	1 mm	+	cc	2.19	III
Lasa	LA2	inequigranular-interlobate	1 mm	+	cc	1.57	III
Palisandro	P1	equigranular-interlobate	300 μm	+	do	2.85	II
Rosa Estremoz	RE	equigranular-polygonal	1.5 mm	+	cc	1.59	III
Soelk	SK1	inequigranular-interlobate	1.25 mm	+	cc	2.94	III
Soelk	SK2	inequigranular-interlobate	1.5 mm	+	cc	3.06	III
Sterzing	ST	inequigranular-interlobate	2.6 mm	+	cc	3.42	III
Wachau	W1	seriate-interlobate	1 mm (250–500 μm)	–	cc	2.09	III
Wachau	W2	seriate-interlobate	1–1.5 mm (500 mm)	–	cc	2.38	III

The commercial name and the abbreviation (abbr.) used in the present study are shown as well as the general fabric, grain size, shape preferred orientation (SPO) composition (comp.: cc, calcitic; do, dolomitic), c-axis maximum in multiples of random distribution (mrd) and thermal dilatation type (TD-type). For marbles with different grain sizes, the second grain size is given in parentheses.

experimental setup see Ullemeyer *et al.* 1998). Based on the neutron diffraction measurements quantitative texture analysis was carried out by means of the iterative series expansion method (Dahms & Bunge 1989). In this method, the texture is described by the coefficients C of spherical harmonic functions. From the C coefficients, anisotropic physical rock properties like elastic wave velocities or thermal dilatation may be easily modelled by averaging the single crystal properties over all observed orientations (e.g. Siegesmund & Dahms 1994). Thus, it is reasonable to assume that the intrinsic properties of a polycrystal are between the maximum and the minimum value of the single crystal. To evaluate the tensorial properties for a second-order quantity of a textured rock the Voigt, Reuss or Hill averaging techniques can be applied (Voigt 1928; Reuss 1929). In this study the Voigt approximation was used. However, the existence and the effect of pre-existing microcracks and grain boundaries is not considered in this model calculation.

The shape preferred orientation was quantified by a semi-automated image analysis method (Duyster 1991). Hand drawn images of grain boundaries of representative cross-sections with respect to the sample coordinate system are scanned and vectorized to determine quantified shape parameters. The quantified shape fabric parameters are given as the characteristic grain boundary orientation plotted in a rose diagram parallel to the three orthogonal sections (Fig. 3).

Rock samples, microfabrics and texture

Eighteen different commercial types of marble have been investigated. They are from Italy (Carrara, Lasa, Sterzing), Greece (Diamant, Arabella, Gitano, Thassos, Volakas, Palisandro), Portugal (Rosa Estremoz), Poland (Grosskunzendorf) and Austria (Soelk, Wachau) and have been widely used as building stones in the past as well as at present. Mineralogically all samples belong to calcitic and dolomitic marbles (Arabella, Thassos and Palisandro) with quartz, biotite, muscovite, phlogopite and ore minerals as accessory phases. The most important characteristics of the fabric elements are summarized in Table 1.

The average grain size, which was calculated from microscopical observations or from the digitized images of the grain boundaries, ranges from 50 μm (Gitano) up to 3 mm (Diamant). All samples are also characterized by a large variation in the shape fabric. The grain boundary orientation given for the xy-, xz- and yz-planes may differ from a more or less random distribution to a distinct planar or linear shape fabric. An example for a random distribution is the Arabella marble, while most of the other marbles (e.g. Soelk, Thassos and Carrara) exhibit a shape preferred orientation (Fig. 3). A more detailed discussion of the fabric is given for

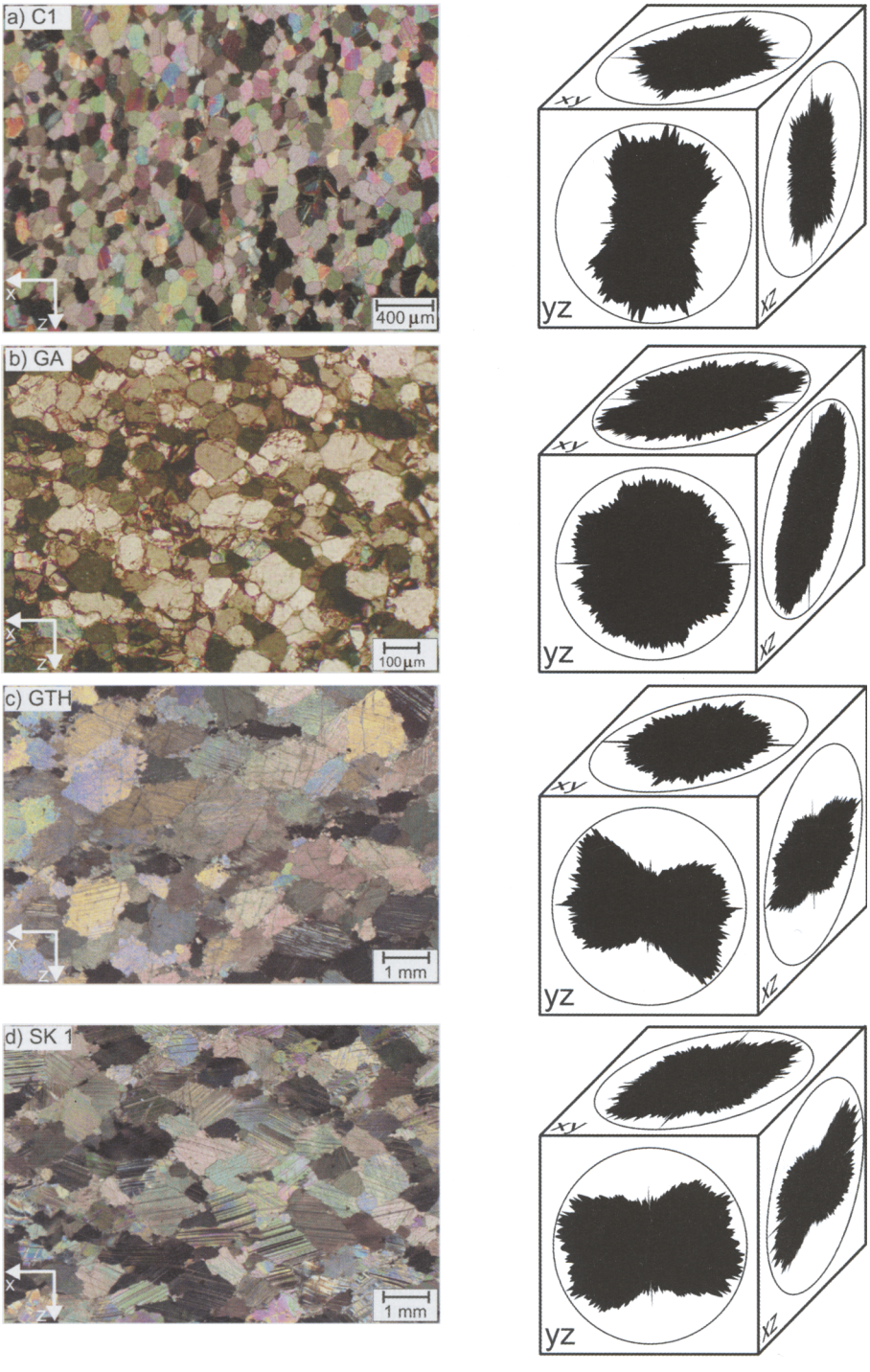

Fig. 3. Microfabric of the marbles investigated: (**a**) Carrara marble (C1), (**b**) Arabella marble (GA), (**c**) Thassos marble (GTH) and (**d**) Soelk marble (SK1). The microfabric is shown in the xz-section of the structural reference frame (left column); the preferred orientation of grain boundaries is shown for all mutually perpendicular planes (right column).

Thassos, Arabella, Soelk and Carrara marbles because they exhibit remarkable differences in the thermal dilatation behaviour. The shape of the grain aggregates can generally be classified between equigranular-polygonal and inequigranular-polygonal in the sense of Moore (1970).

Since a dolomitic composition may have an influence on the durability of marbles, dolomitic and calcitic marbles were compared. Carrara (calcite) and Arabella (dolomite) are fine grained marbles with more or less straight grain boundaries (foam structure). In contrast, Thassos and Soelk are more coarse grained, while the grain boundaries can be characterized as equigranular-interlobate and inequigranular-interlobate. The much higher irregularity of the lobate grain boundaries is clearly shown in Figure 3. Thassos and Soelk exhibit two sets of conjugate planar fabrics with an opening angle of around 50°, which are slightly asymmetrically disposed to the foliation. These fabrics can be easily observed in thin sections and in the corresponding grain boundary surfaces (see Fig. 3). In summary, the grain boundary geometry or the grain interlocking for all marbles ranges between equigranular-polygonal (Rosa Estremoz) up to seriate-interlobate (Gitano) with a slight tendency to be inequigranular-amoeboid (Wachau). This implies that the metamorphic and deformation history over geologically long time spans that control the development of the rock fabrics was quite different for the samples with different fabric types. Recrystallization processes, for instance, may control the grain size and the configuration of grain boundaries. The evidence for grain boundary migration recrystallization is the presence of highly irregular grain boundaries. The driving force is the difference in the dislocation density resulting in a bulging of the grain boundaries into crystals with the higher dislocation density (Gottstein & Mecking 1985). In other cases, subgrain recrystallization may lead to an equilibrium fabric of polygonal crystals with interfacial angles of approximately 120° (Carrara or Arabella). From the mechanical point of view it seems to be clear that a decrease in grain boundary energy is correlated with the decrease in strength of a polycrystalline material.

Besides other processes (for a review see Skrotzki 1994) deformation may be responsible for the development of a lattice preferred orientation (here referred to as texture) which also has a significant influence on physical properties and their directional dependence (e.g. Siegesmund & Dahms 1994; Kocks *et al.* 2000). All samples were analysed with respect to their textures. Leiss & Ullemeyer (1999) discussed the fundamental texture types of calcite and dolomite which are found in nature. In summary, they can be described by a rotating single crystal with the c-axis or a-axis as the rotation axis, respectively. These c-axis and a-axis fibre types can combine to form intermediate texture types. The c-axis and a-axis pole figures for Thassos, Arabella, Soelk and Carrara are illustrated in Figure 4a–d. Usually a single c-axis maximum, which is in most cases elongated to an oval-shaped pattern, can be observed. According to the calcite crystallography the a-axis poles are arranged on a great circle around the c-axis pole density maximum. The maximum pole density is highly variable. The maximum of the c-axis distributions varies from 1.4 mrd (Carrara) to 7.0 mrd (Thassos) (mrd = multiples of random distribution). The latter maximum of (001) indicates a strong texture and, consequently, a pronounced anisotropy of the physical properties must be expected. In order to characterize the textures of all 18 samples, the tensor shape T calculated from the pole figure tensor is applied to describe the different c-axis concentrations (Jelinek 1981). It varies from 1 (perfectly planar) to –1 (perfectly linear). The shape factor T calculated from the pole figure tensor characterizes the texture differences very well. It covers the range from $T = -0.859$ (Wachau) to $T = 0.881$ (Rosa Estremoz) indicating a well-pronounced cluster-like and a moderate girdle-like shape of the intensity distribution as the extreme cases (Fig. 5). Extremely planar c-axis distributions (i.e. complete gridles) are not observed. The maximum intensity, obtained from a simplified texture reproduction with $L = 2$ ranges from 1.4 to 7.0 (Table 1).

Results

Thermal expansion as a function of temperature

The thermal expansion coefficients α of all marbles investigated show a more or less pronounced directional dependence of α (Fig. 6). The directional dependence is weak for the C1 and GA marble and it is very pronounced for the GTH and SK1 marble (see Table 1 for abbreviations). However, it is not only the thermal dilatation coefficient that may be directionally dependent; the residual strain also can be a parameter which varies in magnitude and directional dependence (Fig. 6). On the basis of this extended experimental data set, the thermal

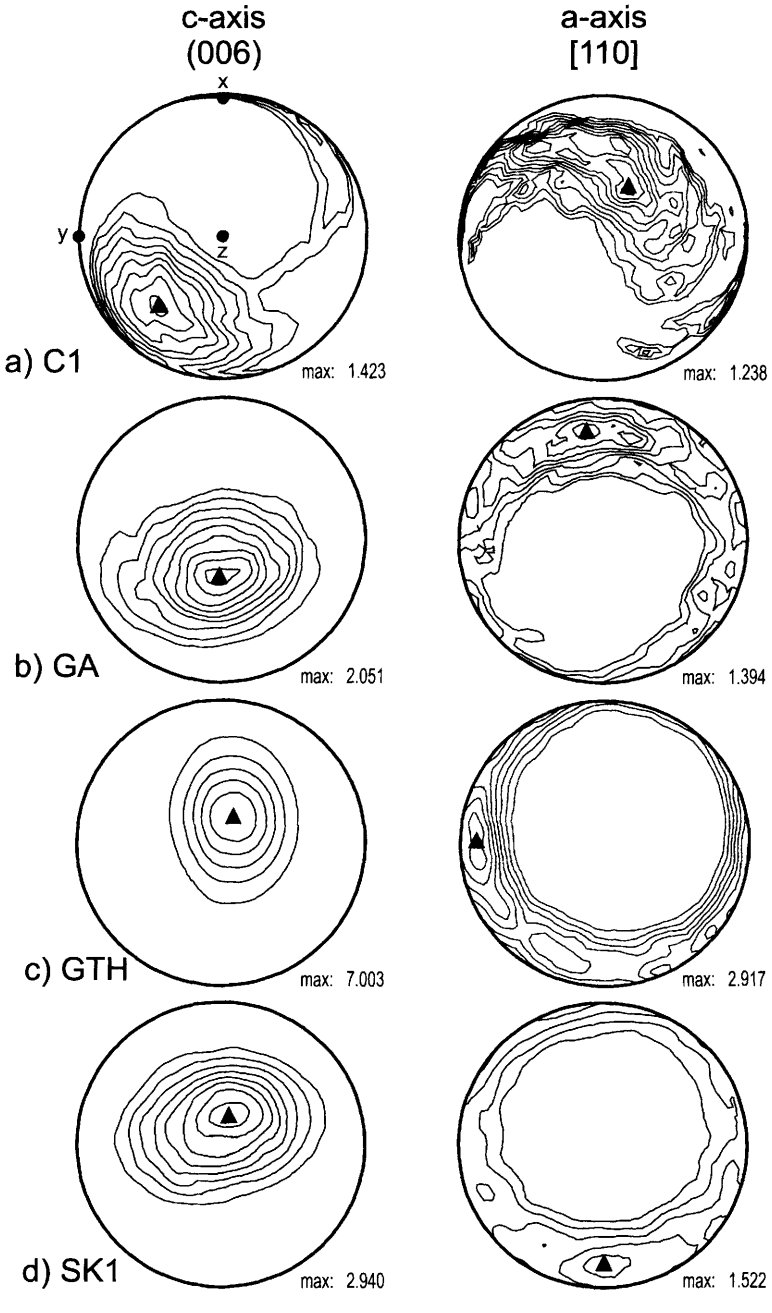

Fig. 4. Texture of the marbles investigated: (**a**) Carrara marble (C1), (**b**) Arabella marble (GA), (**c**) Thassos marble (GTH) and (**d**) Soelk marble (SK1). The c-axis (left column) and a-axis (right column) distributions are shown. The isolines are given as multiples of random distribution (mrd) varying between 1 mrd and the maximum intensity (max), which is marked with a triangle (equal area projection, lower hemisphere). The coordinates of the structural reference frame are shown in (a).

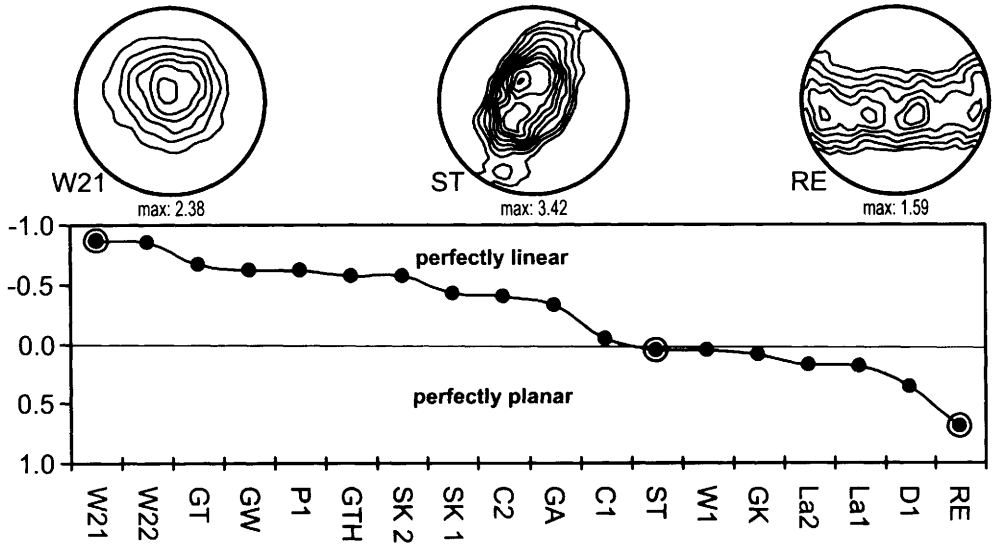

Fig. 5. Variation of texture patterns: the shape factor T as a function of marble type. Examples of pole figures for marbles with linear (W21), neutral (ST) and planar (RE) c-axis distributions are given at the top of the graph (isolines in mrd, equal area projection, lower hemisphere).

expansion versus temperature relationships can be classified into different groups. The samples TH, GA, SK1 and C1 are used as examples to illustrate this interdependence for the directions parallel to the x-, y- and z-direction. The different types can be summarized as follows:

Type I: isotropic α and large isotropic residual strain
Type II: anisotropic α and no or a small isotropic residual strain
Type III: anisotropic α and anisotropic residual strain

Type I. The curves for the Carrara marble clearly exhibit a weak directional dependence of both α and the residual strain. The magnitude of the residual strain is dependent on the destination temperature. The curves for the first, second and third ramp show a successive increase in residual strain. The final result is a permanent expansion of the sample of about 0.2 mm/m. This value corresponds to the summed contribution of all residual strains observed in the preceding ramps. The Arabella marble shows a similar behaviour, but a slightly smaller permanent expansion (about 0.1 mm/m).

Type II. The marble from Thassos is, according to its strong texture, very anisotropic but shows almost no residual strain. Thus, it may be regarded as a marble which is relatively resistant against thermal degradation. The curves show an almost linear thermal expansion and, due to an overlapping of the curves, the individual ramps are hard to discern. Subtypes of this behaviour (e.g. GT, P1) show a small isotropic residual strain.

Type III. The Soelk marble shows both a strong directional dependence of α and the residual strain. A larger residual strain is observed parallel to the z-direction than in the other directions. After the first ramp, the residual strain is very small. It increases significantly in the second and third ramp (see Fig. 6). This effect can best be seen when the z-direction is considered. After the fourth ramp no residual strain is observed. It can be concluded that a certain thermal degradation is monitored by a reinforced gradient of the curves after a certain temperature is reached, corresponding to an increase of α in this part of the curve. A clear directional dependence of the residual strain is also observed for the Wachau marble, but the magnitude is smaller for this marble.

In principle, all marbles investigated can be assigned to these types of thermal behaviour (see Table 1).

Determination of thermal degradation

The Soelk marble is used as an example to illustrate thermal degradation in detail (Fig. 6e, f).

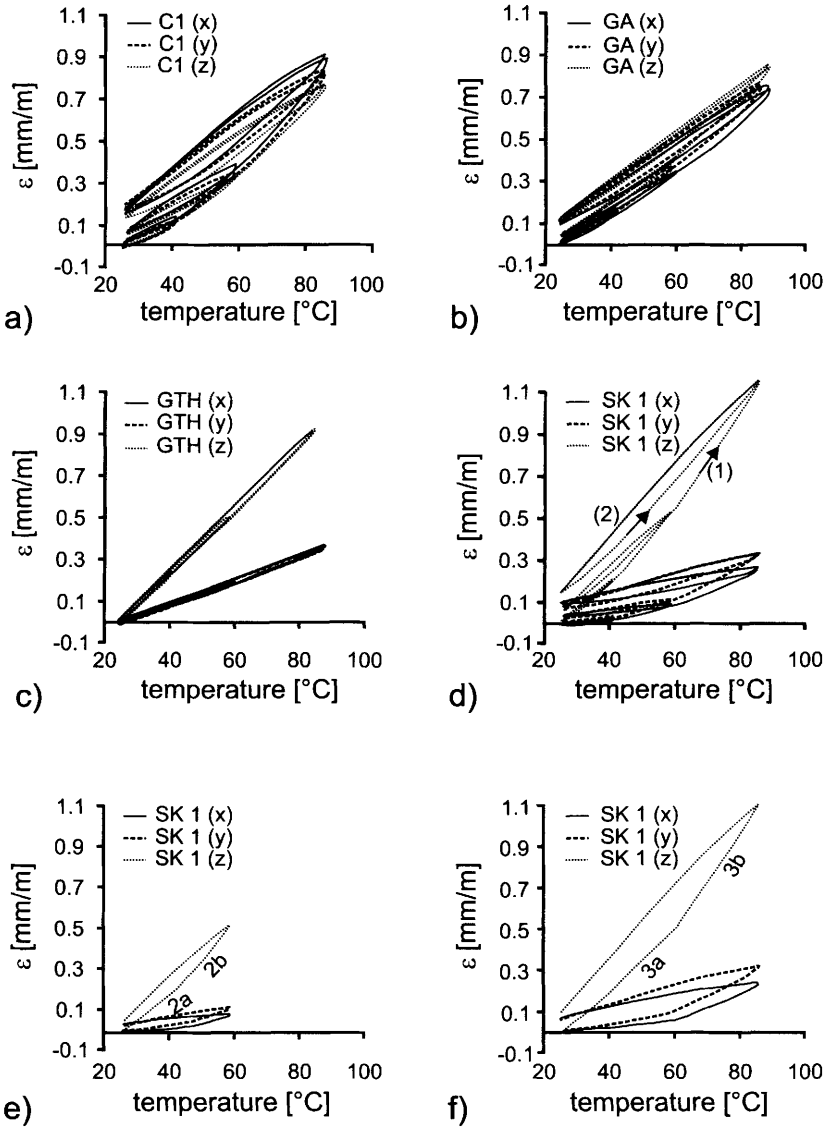

Fig. 6. Thermal dilatation (ε) as a function of temperature: (**a**) Carrara marble (C1), (**b**) Arabella marble (GA), (**c**) Thassos marble (GTH) and (**d**) Soelk marble (SK1). The curves give an overview on all the thermal cycles (ramps) investigated. The final residual strain corresponds to the total contribution of all temperature cycles. (**e** and **f**) Specific examples for the second (e) and third (f) ramps for the SK1 marble (x-, y-, z-direction). In (d) the expansion curves for ramp 3 (1) and ramp 4 (2) at increasing temperature are marked by arrows.

Therefore, the data obtained for the second and third ramp up to 60°C and 85°C, respectively, are used. In the second ramp (Fig. 6e), the curves exhibit a small slope until the temperature of the first ramp (40°C) is reached. In the second part of the curve, the slope increases. The same relationship applies for the third ramp, where an increase in the slope is observed at 60°C, i.e. at the destination temperature of ramp 2. An example for the increase in α associated with thermal microcracking can be given for the z-direction (i.e. maximum dilatation direction), where α increases from 13×10^{-6} (ramp 3a) to 22×10^{-6} (ramp 3b).

Buffering of pre-existing microcracks

It is not unequivocally true that a change in α is only associated with an increase in thermal degradation. The gradient in the first part of the curves can also be smaller when a buffering of pre-existing microcrack systems has to be considered (e.g. Leiss & Weiss 2000). That applies to marbles which are already degraded or which show, as a consequence of their complex geological history, pre-existing microcracks.

Direct evidence for the first cause can be drawn from the experimental data (Fig. 6d) of the Soelk marble using the fourth ramp. In the z-direction, the gradient of the curve is different in the first and second part of the curve, even if no residual strain is observed. Thus, there must be a buffering by pre-existing crack systems. The 'buffering effect' of the Soelk marble in this specific direction (z-direction) in the fourth ramp is relatively small compared to the strong thermal degradation of this marble observed in the previous ramps.

Initiation of thermal degradation

Since the starting temperature for a thermal degradation of marble is supposed to be a characteristic of the specific marble type, it is necessary to have a look at the behaviour of the marbles in the different ramps. For most of the marbles, a very weak residual strain is observed after the first ramp up to 40°C. The values are in the range of the detection limit, i.e. around 0.02 mm/m. In the second ramp up to 60°C the residual strain generally increases. While the C1, C2 and GK marbles reach a residual strain of about 0.05 mm/m, indicating a thermal degradation at relatively low temperatures, the other marbles show values between 0.01 and 0.04 mm/m. In the third ramp, almost all marbles show a residual strain larger than 0.05 mm/m. Exceptions are GT, GTH, P1, W1 and W2. Thus, the latter marbles seem to be rather stable in terms of thermal degradation. In the fourth ramp, the residual strain vanishes for all of the marbles, i.e. no further thermal degradation occurs. The residual strain is generally smaller than observed in the first ramp.

Anisotropy of the thermal dilatation: intrinsic

A compilation of all marbles investigated using the data from the third ramp gives an overview of the particular properties described above. The data of this ramp are used, since almost all marbles show a residual strain at this temperature level and a strong fabric-induced directional dependence of the dilatation coefficient α (Fig. 7). The variation of α is shown as a function of the first and second part of the curve. As mentioned above, the first part of the curve is supposed to be controlled by the intrinsic properties, while the second part of the curves show the interaction between intrinsic properties and thermal degradation. The latter factor may also show a directional dependence when a preferred direction of microcracking is observed.

The weakest variation of α calculated from ramp 3a is observed for the C2 marble, and a very strong directional dependence is observed for the Soelk marble. The α-values for the first part of ramp 3 vary in a wide range from almost zero (Lasa, Rosa Estremoz and Sterzing marbles) to a value of about 15×10^{-6} K^{-1} (Thassos marble). The equivalent expansion associated with an observed α for a 1 m marble slab can be directly determined from Figure 7b. These values have to be regarded as being close to the intrinsic properties, since only the parts of the curves before thermal degradation starts have been evaluated.

Anisotropy of the thermal dilatation: thermally degraded

The second part of the curves gives completely different information. In general, all α-values are higher than those of ramp 3a (Fig. 7a). This indicates that a certain amount of thermal degradation occurred. The GTH marble shows a very small difference in α between ramps 3a and 3b, while it is very pronounced for the C2 marble. For the RE marble, the anisotropy of the thermal dilatation is enlarged in ramp 3b giving evidence for a strong directional dependence of thermal degradation. For some marbles the variability of α at different sample directions is smaller (e.g. GT) or equal in ramps 3a and 3b indicating a uniform crack nucleation. The magnitude and directional dependence of the residual strain associated with the third ramp is shown in Figure 8.

Magnitude of thermal degradation

The residual strain of a sample is characteristic for the degradation of a marble as a consequence of thermal treatment. For a fabric-dependent comparison of thermal degradation, the residual strain associated with ramp 3 is used. This ramp shows a magnitude of residual strain which is clearly above the experimental

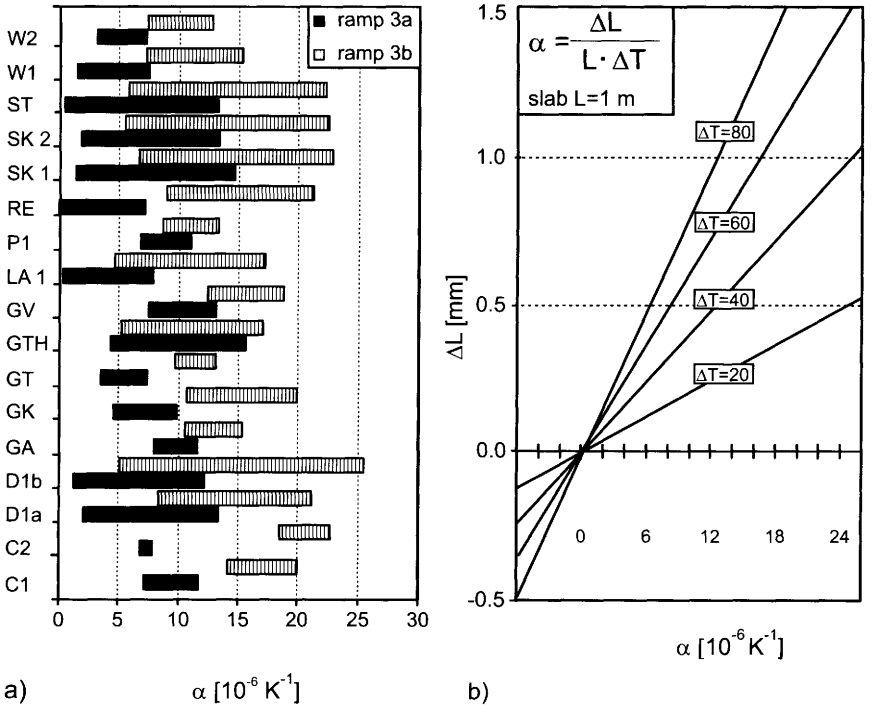

Fig. 7. Variation of the thermal dilatation coefficient as a function of marble type. (**a**) The coefficient of thermal expansion is shown for the first part of the curve (black) and the second part of the curve (hatched) according to the observations described in Figure 6f. (**b**) The expansion of a 1 m marble slab as a function of α for different temperature intervals is shown based on the given formula.

resolution. Thus, these values can be evaluated with a high degree of confidence.

Generally, the residual strain varies from almost zero (GTH) to around 0.2 mm/m for C2. Another extremely deteriorated specimen comparable to C2 is the RE marble, which shows a very high residual strain of about 0.15 mm/m. Two dolomite marbles (GTH, P1) show a very small proneness to thermal weathering. However, most of the marble types investigated are in the range of about 0.05 to 0.1 mm/m. All these values concur quite well with the observed increase of α as a consequence of thermal treatment (cf. Fig. 7).

There is clear evidence that the grain size does not significantly influence the residual strain, even if there is a slight tendency towards a higher residual strain for samples with small grain sizes (Fig. 8). This is even more surprising, since marbles with a larger grain size predominantly exhibit interlobate fabrics, while the finer grained marbles predominantly show polygonal fabrics. An exception is the RE marble with a polygonal fabric and a large grain size.

It can be summarized that a more or less pronounced directional dependence of the residual strain is a general property of all marbles investigated. The start, the magnitude and directional dependence of the residual strain cannot be simply assigned to one fabric property (e.g. the grain size). A combination of all fabric parameters must be considered to understand thermal degradation in marble.

Directional dependence of thermal degradation

In order to quantify the directional dependence of the residual strain, the Soelk marble is used as an example. There is a clear difference between both values (α and the residual strain) at different sample directions. The strong directional dependence of α is obvious considering the strong texture of this marble (see Fig. 4d). For ramp 3b, a strong increase of the slope indicates a certain thermal degradation. To check the relationship between texture-induced and

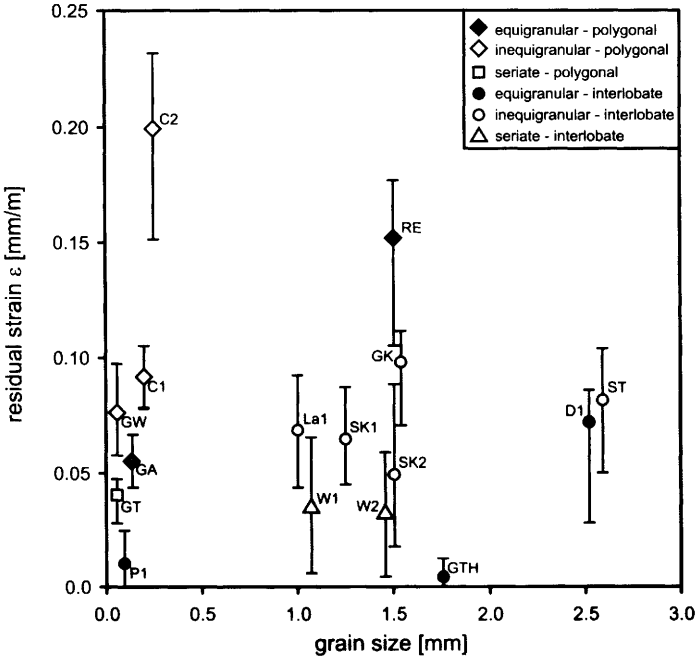

Fig. 8. Residual strain of different marbles as a function of grain size. The maximum and minimum values are given as error bars, the average is calculated from measurements at six independent sample directions. The different fabric types (polygonal, interlobate etc.) are indicated by symbols; dolomite marbles are marked by grey filled symbols.

grain-fabric-induced thermal dilatation the following approach was taken.

At first, the texture-based pole figure of α was calculated. The calculation of second rank tensorial properties like thermal expansion based on textures is described in detail in Siegesmund & Dahms (1994). The basic principle is that the single crystal properties are averaged over all measured orientations. It clearly shows a maximum of α for the z-direction and a minimum parallel to the x-direction (Fig. 9a). A very similar pole figure is obtained, when the almost linear slope of the curves is used for the calculation of the experimentally determined α (Fig. 9b). Therefore, experimental data have been used from six independent directions. The experimentally observed values agree quite well with the modelled ones. For ramp 3b an increase in the slope of the curves concurring with an increase in the dilatation coefficient α is observed, so the difference between α in ramps 3a and 3b can be used to determine the direction of preferred thermal degradation (Fig. 9c). It is obvious that for the Soelk marble the strongest degradation occurs parallel to the c-axis maximum, i.e. perpendicular to the z-direction of the structural reference frame. This can be explained by the observed shape anisotropy of this marble which shows a preferred orientation of grain boundaries perpendicular to the z-directions. A preferred alignment of frequently occurring twin-planes parallel to the foliation may also be of importance (see Fig. 3d) because coarse grained marbles may show a thermal degradation at inter- and intragranular planes while fine grained marbles are predominantly degraded along the grain boundaries (Ruedrich *et al.* 2002).

Intrinsic versus extrinsic anisotropy

A basic question for the comparison of thermal behaviour of the different marbles is whether the anisotropy of α, here referred to as $A = \alpha_{min} / \alpha_{max}$, observed in the experiments is closely linked to the texture. This effect can be best documented when the experimentally determined values (A_{exp}) are shown as a function of calculated (A_{mod}) data. Experimental values are shown for the first part (ramp 3a) and the second part (ramp 3b) of one thermal cycle. A low anisotropy in the graph is characterized

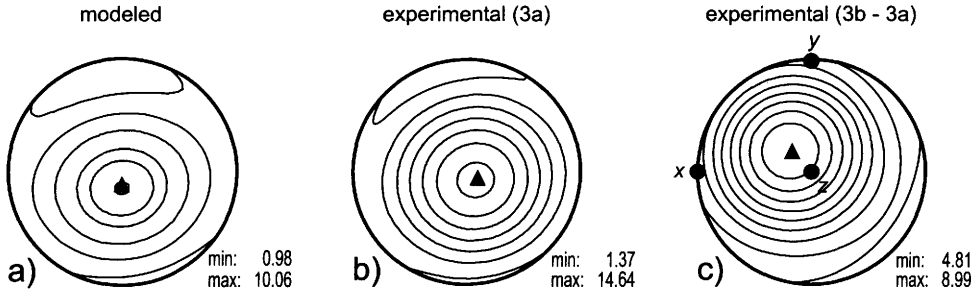

Fig. 9. Texture-induced and experimental dilatation. (**a**) Modelled distribution of the texture-based α; (**b**) directional dependence of the experimentally determined α from ramp 3a; (**c**) increase of α at ramp 3b.

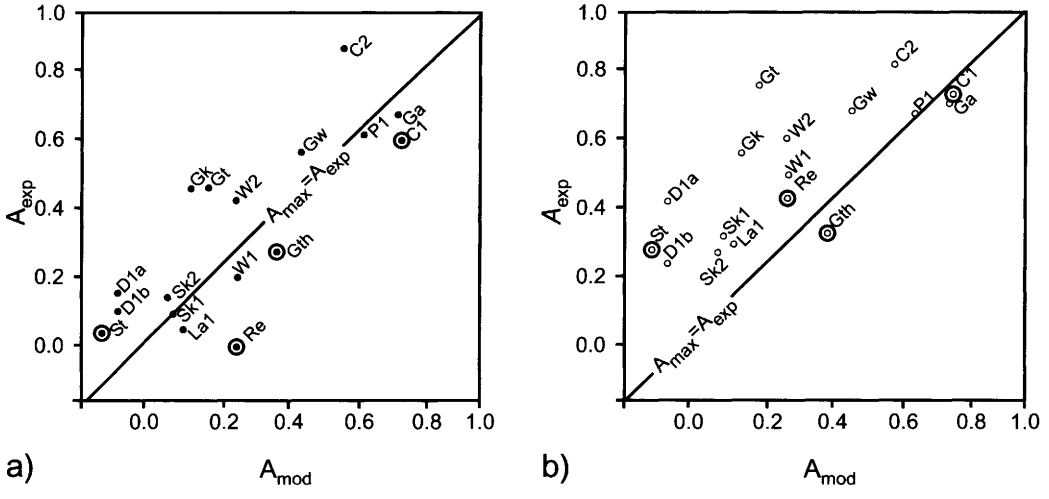

Fig. 10. Anisotropy of experimental thermal dilatation A_{exp} ($A = \alpha_{min}/\alpha_{max}$) as a function of the modelled thermal dilatation A_{mod}. (**a**) A_{exp} calculated from ramp 3a; (**b**) A_{exp} calculated from ramp 3b. The marble types which are described in the text are outlined.

by a value close to 1, while a pronounced anisotropy results in values smaller than 1. There is a general agreement between A_{exp} and A_{mod} (Fig. 10). Samples with a weakly calculated anisotropy exhibit a weak experimental anisotropy and vice versa, when the values calculated for the linear part of the experimental data are considered. The experimental values for the second part are more scattered, which can be taken as an indication that the thermal degradation of a particular marble is controlled not only by the texture but by the complete grain fabric. A few examples may illustrate this behaviour more explicitly (the examples are outlined in the graph). The C1 marble shows a weak anisotropy in both parts of the curve. This indicates that the thermal degradation is uniformly distributed over all orientations. The ST marble shows a stronger anisotropy in the first part of the ramp (Fig. 10a) than in the second part. Thus, the intrinsic anisotropy must be higher and the thermal degradation must be more uniform. The RE marble shows the opposite effect. A stronger anisotropy in the second part than in the first part of the ramp indicates strongly direction-dependent thermal degradation. The GTH marble shows a clear coincidence of the values in both diagrams. Thus, its thermal degradation must be very small or very uniform. This could be shown in Figure 8 for this marble. Consequently, the correlation between A_{exp} and A_{mod} can be used to visualize both the

anisotropy of the thermal dilatation coefficient and the change in α as a consequence of thermal degradation.

Discussion and conclusions

There are many factors supposed to influence thermal degradation of marble. The rock fabric, i.e. composition, grain size, grain shape anisotropy, grain boundary morphology and texture, significantly triggers the proneness to thermal weathering of a marble (e.g. Siegesmund *et al.* 2000*b*). The effect of the different fabric parameters can be summarized as follows.

(1) The modal composition is an important factor for the thermal properties of a marble, since the thermal expansion behaviour is at least partially controlled by the single crystal properties. Both calcite and dolomite show an extreme directional dependence of α at different crystallographic directions. Parallel to the c-axis, both minerals show an α value of about $26 \times 10^{-6}\,K^{-1}$. However, parallel to the a-axis calcite shows a negative α value of about $-6 \times 10^{-6}\,K^{-1}$ while the corresponding value for dolomite is about $6 \times 10^{-6}\,K^{-1}$. Thus, even strongly anisotropic dolomite marbles will not show any contraction with increasing temperature as shown for the GTH marble. Since the GA (dolomite) and C1 (calcite) marble show a similar thermal degradation, the residual strain is likely not to be controlled exclusively by the composition. However, other mechanical properties like compressive and tensile strength of calcite and dolomite marbles may vary significantly according to the different Young's modulus and shear modulus of these minerals (Bass 1995). Accessory minerals like mica may have more effect on other weathering processes (e.g. Ondrasina *et al.* 2002).

(2) The grain size cannot be the most important factor for marble degradation (see Fig. 7). Marbles with a large grain size exhibit the same magnitude of residual strain as marbles with a small grain size. A similar relationship was also proposed by Tschegg *et al.* (1999). This correlation applies even for extraordinarily deteriorated examples like C2 and RE. However, thermal degradation is a strongly direction-dependent parameter, and thus, its directional dependence must be taken into account.

(3) The grain shape anisotropy significantly triggers thermal degradation, as shown for the SK1 marble. This observation is supported by the observations of Ruedrich *et al.* (2002) for a weathered Prieborn marble (see also Siegesmund *et al.* 2000*b*). Thus, since grain boundary cracking is the most prominent factor for marble degradation, a substantial part of the observed directional dependence of residual strain must be attributed to shape fabrics.

(4) The grain boundary morphology, i.e. the irregularity of grain boundaries, does not play such an important role as was previously assessed. Marbles with interlobate fabrics as well as marbles with polygonal fabrics may show a residual strain after thermal treatment. An exception may be the WA marble, which shows amoeboid (i.e. highly irregular) grain boundaries leading to a very small residual strain. However, the large amount of mica and a clearly inequigranular grain size distribution may accommodate a certain amount of thermally induced stress that does not exceed the threshold of cohesion. Thus, further studies must be performed to quantify and localize a fabric-dependent deterioration.

(5) The texture clearly determines magnitude and directional dependence of α, since there is a general agreement between calculated (texture-based) and experimentally determined anisotropies. Thermal degradation changes this relation, i.e. the anisotropies increase or decrease according to a coincidence or contrariness of thermal degradation and intrinsic dilatation, respectively. A general observation is that the maximum of thermal degradation is closely linked to the c-axis maximum. A deviation in this behaviour can be traced back to shape preferred orientations oblique to the c-axis maximum. However, the individual grain-to-grain orientation may be of importance. Tschegg *et al.* (1999) found that large internal stresses, leading to thermal microcracking when the threshold of cohesion is exceeded, are caused by an almost random orientation of the grains. The specific relationship of this almost random orientation may also be valid for strongly textured marbles at certain sample directions. This could cause a directional dependence of thermal degradation even if no clear shape preferred orientation is observed. However, this assumption must be validated in the future by single grain texture measurements and model calculations.

(6) Pre-existing microcrack systems may be of importance as well. Siegesmund *et al.* (2000*b*) have shown that a change in the anisotropy patterns between modelled and experimentally determined values may be explained by pre-existing microcracks, resulting from a complex geological history.

In summary, it can be stated that there is a clear fabric dependence of residual strain after thermal treatment and, thus, of thermal degradation. Thermally induced microcracks lead to a

residual strain after heat treatment and, thus, to a deterioration of the rock's quality. However, the fabric cannot be reduced to one or a small number of parameters (e.g. only grain size, grain shape etc.). The thermal degradation of a marble is controlled by an interaction of all fabric parameters.

We gratefully acknowledge the help of E. Tschegg and K. Ullemeyer for their support with the experimental run of the thermal expansion measurements and the neutron texture measurements. The study was supported by the Deutsche Forschungsgemeinschaft with the grants Si 438/10-1, 2 (Heisenberg-Fellowship) and Si 438/13-1. We extend our thanks to the reviewers F. Zezza and H.R. Wenk for their constructive reviews which helped to improve the paper.

References

BASS, J. D. 1995. Elasticity of minerals, glasses, and melts. *In*: AHRENS, T. J. (ed.) *Handbook of Physical Constants*. American Geophysical Union, Washington, DC, 45–63.

BATTAGLIA, S., FRANZINI, M. & MANGO, F. 1993. High sensitivity apparatus for measuring thermal expansion: preliminary results on the response of marbles. *Il Nuovo Cimento*, **16,** 453–461.

BORTZ, S. A., ERLIN, B. & MONK, C. B., JR. 1988. Some field problems with thin veneer building stones. *In*: DONALDSON, B. (ed.) *New Stone Technology, Design, and Construction for Exterior Wall Systems*. American Society for Testing and Materials, Philadelphia, Special Technical Publication **996**, 11–31.

DAHMS, M. & BUNGE, H.-J. 1989. The iterative series-expansion method for quantitative texture analysis, I. General Outline. *Journal of Applied Crystallography*, **22**, 439–447.

DUYSTER, J. 1991. *Strukturgeologische Untersuchungen im Moldanubikum (Waldviertel, Oesterreich) und methodische Untersuchungen zur bildanalytischen Gefuegequantifizierung von Gneisen*. PhD Thesis, University of Goettingen.

FRANZINI, M. 1995. Stones in monument: natural and anthropogenic deterioration of marble artifacts. *European Journal of Mineralogy*, **7,** 735–743.

GRIMM, W. D. 1999. Beobachtungen und Ueberlegungen zur Verformung von Marmorobjekten durch Gefuegeauflockerung. *Zeitschrift der Deutschen Geologischen Gesellschaft*, **150**(2), 195–235.

GRIMM, W. D. & SCHWARZ, U. 1985. Naturwerksteine und ihre Verwitterung an Muenchener Bauten und Denkmaelern Ueberblick ueber eine Stadtkartierung. Bayerisches Landesamtes für Denkmalpflege, Muenchen (Lipp), Arbeitsheft **31**, 28–118.

GOTTSTEIN, G. & MECKING, H. 1985. Recrystallization. *In*: WENK, H.-R. (ed.) *Preferred Orientation in Deformed Metals and Rocks, an Introduction to Modern Texture Analysis*. Academic Press, Orlando, 183–214.

JELINEK, V. 1981. Characterization of the magnetic fabric of rocks. *Tectonophysics*, **79**, 63–67.

KESSLER, D. W. 1919. *Physical and chemical tests of the commercial marbles of the United States*. Technologic Papers of the Bureau of Standards, **123**, Government Printing Office, Washington DC.

KOCKS, U. F., TOMÉ, C. N. & WENK, H.-R. 2000. *Texture and Anisotropy. Preferred Orientations in Polycrystals and their Effect on Materials Properties*. Cambridge University Press.

LASAGA, A. C. & BLUM, A. E. 1986. Surface chemistry, etch pits and mineral-water reactions. *Geochimica et Cosmochimica Acta*, **50**(10), 2263–2379.

LEISS, B. & ULLEMEYER, K. 1999. Texture characterisation of carbonate rocks and some implications for the modeling of physical anisotropies, derived from idealized texture types. *Zeitschrift der Deutschen Geologischen Gesellschaft*, **150**(2), 259–274.

LEISS, B. & WEISS, T. 2000. Fabric anisotropy and its influence on physical weathering of different types of Carrara marbles. *Journal of Structural Geology*, **22**, 1737–1745.

MACINNIS, I. N. & BRANTLEY, S. L. 1992. The role of dislocations and surface morphology in calcite dissolution. *Geochimica et Cosmochimica Acta*, **56**(3), 1113–1126.

MONK, C. B., JR. 1985. The rational use of masonry. *Protocol of the Third North American Masonry Conference*. Construction Research Centre, Civic Engineering Department, University of Texas, 191–227.

MOORE, A. C. 1970. Descriptive terminology for the textures of rocks in granulite facies terrains. *Lithos*, **3**, 123–127

ONDRASINA, J., KIRCHNER, D., SIEGESMUND, S. 2002. Freeze–thaw cycles and their influence on marble deterioration: a long-term experiment. *In*: SIEGESMUND, S., WEISS, T. & VOLLBRECHT, A. (eds) *Natural Stone, Weathering Phenomena, Conservation Strategies and Case Studies*. Geological Society, London, Special Publications, **205**, 9–18.

POSCHLOD, K. 1990. Das Wasser im Porenraum kristalliner Naturwerksteine und sein Einfluss auf die Verwitterung. *Muenchner Geowissenschaftliche Abhandlungen*, **7**, 1–62.

ROSENHOLTZ, J. L.& SMITH, D. T. 1949. Linear thermal expansion of calcite, var. Iceland spar and Yule marble. *The American Mineralogist*, **34**, 846–854.

RUEDRICH, J., WEISS, T. & SIEGESMUND, S. 2002. Thermal behaviour of weathered and consolidated marbles. *In*: SIEGESMUND, S., WEISS, T. & VOLLBRECHT, A. (eds) *Natural Stone, Weathering Phenomena, Conservation Strategies and Case Studies*. Geological Society, London, Special Publications, **205**, 255–272.

REUSS, A. 1929. Berechnung der Fliessgrenze von Mischkristallen auf Grund der Plastizitaetsbedingung für Einkristalle. *Zeitschrift für Angewandte Mathematik und Mechanik*, **9**, 49–58.

SAGE, J. D. 1988. Thermal microfracturing of marble. *In*: MARINOS & KOUKIS (eds) *Engineering Geology of Ancient Works, Monuments and Historical Sites*. Balkema, Rotterdam, 1013–1018.

SCHWARZ, A., LEHLHORN, L., BOUÉ, A. & MANGELS, H. 1991*a*. Bewittertung von Natursteinen mit schadgashaltiger Luft, orientierende Simulationsversuche in einer Doppelklimakammer, Teil 1. *Bautenschutz und Bausanierung*, **14**, 85–97.

SCHWARZ, A., LEHLHORN, L., BOUÉ, A. & MANGELS, H. 1991*b*. Bewitterung von Natursteinen mit schadgashaltiger Luft, orientierende Simulationsversuche in einer Doppelklimakammer, Teil 2. *Bautenschutz und Bausanierung*, **14**, 108–110.

SIEGESMUND, S. & DAHMS, M. 1994. Fabric-controlled anisotropy of elastic, magnetic and thermal properties of rocks. *In*: BUNGE, H. J., SKROTZKI, W., SIEGESMUND, S. & WEBER, K. (eds) *Textures of Geological Materials,* Oberursel (DGM Informationsgesellschaft), 353–379.

SIEGESMUND, S., WEISS, T. & TSCHEGG, E. 2000*a*. Control of marble weathering by thermal expansion and rock fabrics. *19th International Congress on Deterioration and Conservation of Stone*, Venice. Elsevier, Amsterdam, 205–213.

SIEGESMUND, S., ULLEMEYER, K., WEISS, T. & TSCHEGG, E. 2000*b*. Physical weathering of marbles caused by thermal anisotropic expansion. *International Journal of Earth Science,* **89**, 170–182.

SIMON, S & SNETHLAGE, R. 1993. *The first stages of marble weathering, preliminary results after short-term exposure of nine month*. Forschungs-Bericht, (Eurocare-Euromarble EU 496), München (Bayrisches Landesamt für Denkmalpflege) **11/1993**, 37–44.

SKROTZKI, W. 1994. Mechanisms of texture development in rocks. *In*: Bunge, H. J., Skrotzki, W., Siegesmund, S. & Weber, K. (eds) *Textures of Geological Materials*. Oberursel (DGM Informationsgesellschaft), 147–164.

THOMASEN S. E. & EWART C. S. 1984. Durability of thin-set marble. *Third International Conference on Durability of Building Materials and Components*. American Society for Testing and Materials, 313–323.

TSCHEGG, E., WIDHALM, C. & EPPENSTEINER, W. 1999. Ursachen mangelnder Formbestaendigkeit von Marmorplatten. *Zeitschrift der Deutschen Geologischen Gesellschaft*,**150**(2), 283–297.

ULLEMEYER, K., SPALTHOFF, P. L., HEINITZ, J., ISAKOV, N. N., NIKTIN, A. N. & WEBER, K. 1998. The SKAT texture diffractometer at the pulsed reactor IBR-2 at Dubna: experimental layout and first measurements. *Nuclear Instruments & Methods in Physics Research*, **A412/1**, 80–88.

VOIGT, W. 1928. *Lehrbuch der Kristallphysik*. Teubner, Leipzig.

WATSON, B. E. & BRENAN, J. M. 1987. Fluids in the lithosphere; 1. Experimentally-determined wetting characteristics of $CO_2 - H_2O$ fluids and their implications for fluid transport, host-rock physical properties, and fluid inclusion formation. *Earth and Planetary Science Letters*, **85**(4), 497–515.

WIDHALM, C., TSCHEGG, E. & EPPENSTEINER, W. 1996. Anisotropic thermal expansion causes deformation of marble cladding. *Journal of Performance of Constructed Facilities*, **10**, 5–10.

WINKLER, E. M. 1996. Technical note: properties of marble as building veneer. *International Journal of Rock Mechanics, Mineral Science & Geomechanics*, **33**(2), 215–218.

ZEZZA, U., PREVIDE MASSARA, E., MASSA, V. & VENCHIARUTTI, D. 1985. Effect of Temperature on Intergranular Decohesion of the Marbles. *5th International Congress on Deterioration and Conservation of Stone*, Lausanne, Vol. 1, 131–140.